

# New BaBar Results on Rare Leptonic B Decays

Valerie Halyo  
Stanford Linear Accelerator Center  
2575 Sand Hill Rd.  
Menlo Park, CA, 94025  
U.S.A

## 1 Abstract

New preliminary BaBar results for rare leptonic decays  $B^- \rightarrow K^- \nu \bar{\nu}$  and  $B^0 \rightarrow \ell^+ \ell^-$  are reported. Using data collected at the  $\Upsilon(4S)$  with the BaBar detector, no evidence for a signal was found yielding the corresponding upper limits at the 90% confidence level:  $\mathcal{B}(B^- \rightarrow K^- \nu \bar{\nu}) < 9.4 \times 10^{-5}$  for  $50.7 \text{ fb}^{-1}$ ,  $\mathcal{B}(B^0 \rightarrow e^+ e^-) < 3.3 \times 10^{-7}$ ,  $\mathcal{B}(B^0 \rightarrow \mu^+ \mu^-) < 2.0 \times 10^{-7}$  and  $\mathcal{B}(B^0 \rightarrow e^\pm \mu^\mp) < 2.1 \times 10^{-7}$  using  $54.4 \text{ fb}^{-1}$ .

## 2 $B^- \rightarrow K^- \nu \bar{\nu}$

The exclusive decay  $B^- \rightarrow K^- \nu \bar{\nu}$  is characterized by the absence of the long distance contributions and by the fact that the effective Hamiltonian is represented in the Standard Model (SM) by only one operator. In the SM the decay proceeds via the  $W$  box and  $Z$  penguin diagrams as can be seen in fig 1. This mode probes the quark mixing parameter  $|V_{ts}|$ . The SM prediction is  $\mathcal{B}(B^- \rightarrow K^- \nu \bar{\nu}) = 3.8_{-0.6}^{+1.2} \times 10^{-6}$  [1][2] and the previous best limit obtained by CLEO is  $\mathcal{B}(B^- \rightarrow K^- \nu \bar{\nu}) < 2.4 \times 10^{-4}$  [3]. Enhancement beyond the SM can arise from various types of models [4]. The highly constrained models where the existing bounds on other Flavor Changing Neutral Current processes imply that the rate for  $B^- \rightarrow K^- \nu \bar{\nu}$  can not exceed the SM prediction by more than a factor of a few. In this category we have for example the Multi Higgs Doublet Models and the Left Right symmetric models. Enhancement by one or two orders of magnitude can arise from models with an extra vector-like down quark or models with leptophobic  $Z'$  bosons [5]. Last are the unconstrained models where the couplings responsible of enhancing  $B^- \rightarrow K^- \nu \bar{\nu}$  are to a large extent independent of current existing experiment bounds. An example which belongs to this category is supersymmetric models without R-parity.

The presence of two neutrinos in the final state precludes the use of any kinematic constraints on the signal  $B$  meson. The strategy adopted for the BaBar analysis was to look for a charged kaon with momentum  $p^* > 1.5 \text{ GeV}$  in the  $\Upsilon(4S)$  frame

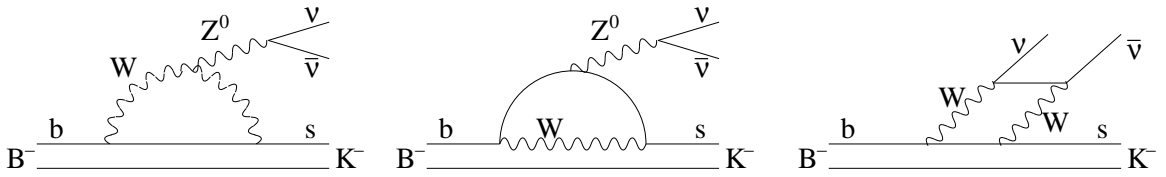


Figure 1: Standard Model Feynman diagrams for  $B^- \rightarrow K^- \nu \bar{\nu}$ .

recoiling against a semileptonic decay  $B^+ \rightarrow \bar{D}^0 \ell^+ \nu(X)$  where X represent either a null or a photon or a  $\pi^0$  from higher mass charm states. The exclusively reconstructed  $B$  meson is referred in the following as the tag  $B$ . The BaBar standard practice of blind analysis was followed to prevent biases. The low multiplicity of the signal decay reduces the combinatorial background in the tag  $B$  reconstruction allowing the semileptonic decay  $B^+ \rightarrow \bar{D}^0 \ell^+ \nu(X)$  to be cleanly reconstructed. The  $\bar{D}^0$  is reconstructed in the  $K^+ \pi^-$ ,  $K^+ \pi^- \pi^- \pi^+$  and  $K^+ \pi^- \pi^0$  modes. This method results in roughly 0.5% of tag reconstruction efficiency. The data used in the analysis consist of  $50.7 \text{ fb}^{-1}$  collected at the  $\Upsilon(4S)$  resonance corresponding to  $56.3 \times 10^6 B\bar{B}$  events and  $6.4 \text{ fb}^{-1}$  collected just below  $B\bar{B}$  threshold. The kinematics for the  $B^- \rightarrow K^- \nu \bar{\nu}$  decays in the simulation is based on the form factor model in [1].

Hadronic events were selected once an electron or muon with a momentum above 1.3 GeV in the  $\Upsilon(4S)$  rest frame was identified. Then  $\bar{D}^0$  candidates were reconstructed in one of the  $K^+ \pi^-$ ,  $K^+ \pi^- \pi^- \pi^+$  and  $K^+ \pi^- \pi^0$  decay modes. The kinematic requirement on the angle between the  $B$  and the reconstructed  $D\ell$ , calculated in the  $\Upsilon(4S)$  frame was used to suppress background and restrict the kinematics of the  $\bar{D}^0 \ell^+$  to be consistent with coming from a semileptonic  $B$  decay. The requirement  $-2.5 < \cos \theta_{B D\ell} < 1.1$  was imposed, using

$$\cos \theta_{B D\ell} = \frac{2 E_B E_{D\ell} - m_B^2 - m_{D\ell}^2}{2 |\vec{p}_B| |\vec{p}_{D\ell}|} . \quad (1)$$

where  $E_B$  and  $|\vec{p}_B|$  are respectively the energy and magnitude of the momentum of the  $B$  meson in the  $\Upsilon(4S)$  frame.

A special double tag sample was used to extract a correction to the efficiency calculated from signal Monte Carlo (MC). The sample was reconstructed by first finding a suitable  $\bar{D}^0 \ell^+$  candidate where the  $\bar{D}^0$  decays to  $K^+ \pi^-$ , and then looking for a second  $D\ell$  candidate in any of the accepted  $\bar{D}^0$  modes. The observed rate of double tags per  $\text{fb}^{-1}$  in the data is  $0.85 \pm 0.11$  times the rate in the simulation leading to a correction to the the signal efficiency by a factor  $0.92 \pm 0.06$  where the uncertainty is taken as a systematic error. The uncertainty in the efficiency of several of the selection criteria were also studied using the double-tagged sample. The total relative uncertainty on the selection efficiency was found to be  $\delta\epsilon/\epsilon = 8.7 \%$  where

the tagging efficiency and ( $E_{\text{left}}$ ) the remaining neutral energy after the tag  $B$  and its daughter were removed contribute the most.

The distribution of events in the search plane defined by the variables<sup>1</sup>  $E_{\text{left}}$  and  $(m_D - m_D^{\text{fit}})/\sigma_D^{\text{fit}}$  is shown in fig 2. We observe 2 events in the signal box, defined by the requirements  $E_{\text{left}} < 0.5 \text{ GeV}$  and  $(m_D - m_D^{\text{fit}}) < 3\sigma_D^{\text{fit}}$ . The expected background from the MC is 2.2 events. The background at present appears to be mostly  $c\bar{c}$  events.

The Poisson upper limit calculated at 90% C.L. without background subtraction is

$$\mathcal{B}(B^- \rightarrow K^- \nu \bar{\nu}) < 9.4 \cdot 10^{-5} \quad (2)$$

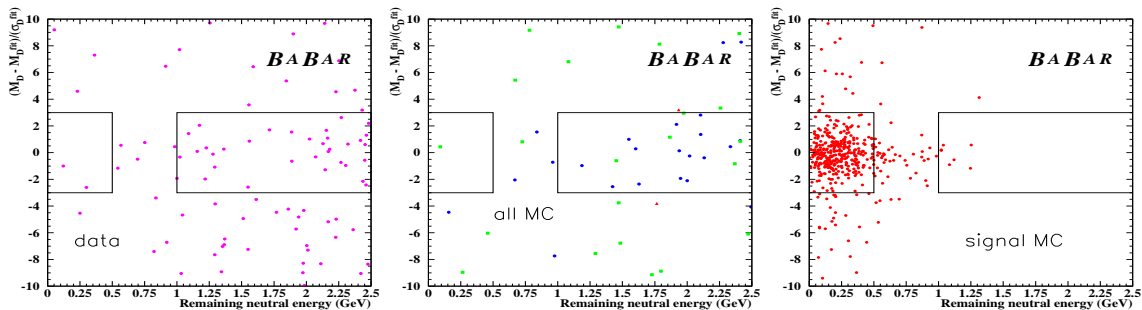


Figure 2: The distribution of events in the  $((m_D - m_D^{\text{fit}})/\sigma_D^{\text{fit}}, E_{\text{left}})$  plane for on-peak data, generic  $B\bar{B}$  and continuum MC and signal MC. In the generic MC plot the blue circles show the contribution from  $B\bar{B}$  events, the green squares show the contribution from  $c\bar{c}$  and the red triangles show the contribution from  $u\bar{u}/d\bar{d}/s\bar{s}$ . The generic MC contributions needs to be scaled by a factor of 1.09, 2.21 and 3.56 for the  $B\bar{B}$ ,  $c\bar{c}$  and  $u\bar{u}/d\bar{d}/s\bar{s}$  contributions respectively to correspond to the on-peak data luminosity.

### 3 $B^0 \rightarrow l^+ l^-$

$B^0 \rightarrow l^+ l^-$  proceeds in the SM through the three dominant  $W$  box and  $Z$  penguin diagrams shown in fig. 3. Even though these diagrams are similar to the one that lead to  $B^- \rightarrow K^- \nu \bar{\nu}$  these decays are further helicity suppressed by factors of  $m_l^2$ . Both  $B^0 \rightarrow l^+ l^-$  and  $B^- \rightarrow K^- \nu \bar{\nu}$  FCNC transitions provide an essential opportunity to test the SM and offer a complementary strategy in the search for new physics by probing the indirect effects of new particles and interactions. The SM theoretical branching ratio predictions are  $1.9 \times 10^{-15}$  for  $B^0 \rightarrow e^+ e^-$ ,  $8.0 \times 10^{-11}$  for  $B^0 \rightarrow \mu^+ \mu^-$  and null for  $B^0 \rightarrow e^\pm \mu^\mp$  although recent neutrino mixing experiment results suggest that the branching ratio would be less than  $10^{-15}$ . To date these decays have not

<sup>1</sup>The quantities  $m_D^{\text{fit}}$  and  $\sigma_D^{\text{fit}}$  are the mean and sigma from Gaussian fits to the  $D^0$  invariant mass spectrum. Separate values are calculated for each  $D^0$  decay mode in data and simulation.  $E_{\text{left}}$  is the remaining neutral energy after the tag  $B$  and its daughter were removed

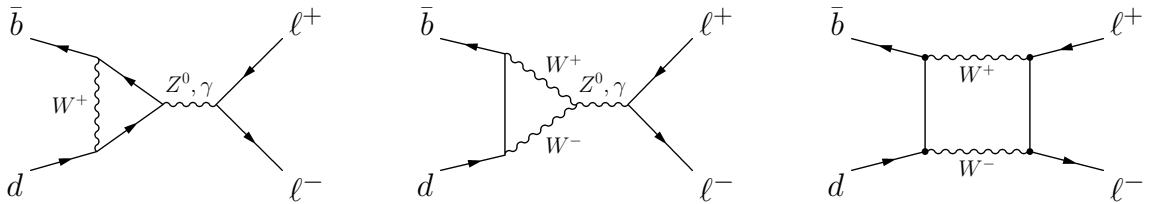


Figure 3: Standard Model Feynman diagrams for  $B^0 \rightarrow \ell^+ \ell^-$ .

been observed and the current best limits from CLEO and Belle are summarized in table 2 [6]-[7]. Since these processes are highly suppressed in the SM they are potentially sensitive probes of physics beyond the SM. Models such as MHDM with Natural Flavor Conservation and large  $\tan\beta$  can give up to an order of magnitude enhancement [8]. The enhancement in models with an extra vector-like down quark can be up to two orders [9]. Large enhancement may also arise from Minimal Supersymmetric Models with large  $\tan\beta$  [10] or Supersymmetric models without R-parity.

The decay  $B^0 \rightarrow l^+ l^-$  offers a very clean experimental signature in the BaBar detector. The two high momentum leptons can be measured precisely and identified with high purity in the detector. Relatively low backgrounds arise from the continuum consisting mostly of non-resonant  $e^+ e^- \rightarrow q \bar{q}$  production where  $q = u, d, s, c$ . The main contribution in the case of  $B^0 \rightarrow e^+ e^-$  is from pairs of real electrons in  $c\bar{c}$  production; the contribution of misidentified hadron-electron pairs is negligible. Two-photon events contribute a significant background. Misidentification of muons is significantly more important in the case of  $B^0 \rightarrow \mu^+ \mu^-$ , as evidenced by an increased background expectation from  $uds$  events. For the  $B^0 \rightarrow \mu^+ \mu^-$  channel, the background from two-photon processes is negligible.

The main measurement criteria are used to suppress different background events. The multiplicity cut  $N_{mult} = N_{Trk} + N_\gamma/2 \geq 6$ ,  $E_\gamma > 80$  MeV suppresses radiative Bhabha events while maintaining a higher efficiency than a simple stringent multiplicity cut. The tracks are restricted to the central region of the detector using a polar angle cut which is efficient in removing QED background due to its strong dependence on the polar angle. As mentioned above, the main background process comes from continuum events which exhibit a two jet structure and produce high momentum approximately back to back tracks satisfying the requirements imposed on our candidate events. Two different shape variables suppress this kind of background:  $|\cos\theta_T| < 0.84$  where  $\theta_T$  is the angle between the thrust axes of the  $B$ -candidate and the rest of the event and the event thrust magnitude  $|T| < 0.9$ . The lepton pair is selected by simultaneous requirements on the energy difference  $\Delta E$  and the energy-substituted mass  $m_{ES}$  defined in the following. The invariant energy difference of the  $B$ -meson candidate and the energy-substituted mass  $m_{ES}$  are calculated as

$$\Delta E = \frac{p_B \cdot p_i - s/2}{\sqrt{s}} \quad m_{ES} = \sqrt{(s/2 + \mathbf{p}_B \cdot \mathbf{p}_i)^2/E_i^2 - \mathbf{p}_B^2} \quad (3)$$

where  $\sqrt{s}$  is the CMS energy,  $p_B$  and  $p_i$  denote the four-momenta of the  $B$ -meson candidate and the initial state.

The signal box is defined in the  $(m_{ES}, \Delta E)$  plane and was obtained for each of the  $B^0 \rightarrow l^+l^-$  mode separately using an upper limit optimization. The size of the signal and Grand Sideband (GSB) was chosen to be roughly  $[+2, -2]\sigma$  of the expected resolution in  $\Delta E$  and  $[+2, -2]\sigma$  for  $m_{ES}$ . In the cases of  $B^0 \rightarrow e^+e^-$  and  $B^0 \rightarrow e^\pm\mu^\mp$ , the signal box size in  $\Delta E$  were relaxed to roughly  $[+2, -3]\sigma$  and  $[+2, -2.5]\sigma$  to account for increased amounts of final state radiation and bremsstrahlung.

The resulting efficiencies for the three  $B^0 \rightarrow l^+l^-$  are given in table 1. The number of events observed in the GSB appears in figure 4. In order to estimate the number of background events in the signal box an unbinned maximum likelihood fit was done using an Argus fit for the  $m_{ES}$  distribution and an exponential fit for  $\Delta E$  distribution. The results are given in table 1. There are three sources of systematic uncertainties: The normalization, the signal efficiency and the background estimate. The systematic uncertainties for the different variables were estimated using a control sample of  $B \rightarrow J/\Psi K_s^0$  with  $J/\Psi \rightarrow \ell^+\ell^-$ . Since there is no control sample for  $B^0 \rightarrow e^\pm\mu^\mp$  the error for  $B^0 \rightarrow e^+e^-$  was assigned to  $B^0 \rightarrow e^\pm\mu^\mp$  and the total systematic errors amount to 8.6%, 5.2% and 8.6% for  $B^0 \rightarrow e^+e^-$ ,  $B^0 \rightarrow \mu^+\mu^-$  and  $B^0 \rightarrow e^\pm\mu^\mp$  respectively where the main contribution is from  $m_{ES}$  and  $\Delta E$ .

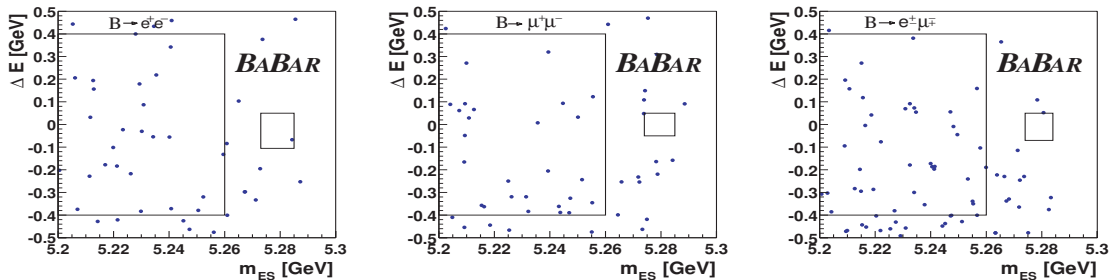


Figure 4: Unblinded  $(m_{ES}, \Delta E)$  distributions with 25, 26 and 37 events in the GSB for  $B^0 \rightarrow e^+e^-$ ,  $B^0 \rightarrow \mu^+\mu^-$  and  $B^0 \rightarrow e^\pm\mu^\mp$  respectively.

After unblinding, we observed 1 event in the signal box for  $B^0 \rightarrow e^+e^-$  and none for the rest of the channels are summarized in table 1. The unbinned  $(m_{ES}, \Delta E)$  distributions for the three channels are shown in figs [4]. The observation are compatible with the expected background. We do not perform background subtraction for the determination of the branching fraction (upper limit).

The upper limits on the branching ratios for  $B^0 \rightarrow l^+l^-$  obtained at the 90% confidence level are summarized in table 1.

Channel	$N_{exp}$	$N_{obs}$	$N_{BG}$	$\varepsilon[\%]$	UL (90% CL)
$B^0 \rightarrow e^+e^-$	$1 \times 10^{-8}$	1	$0.60 \pm 0.24$	$19.3 \pm 0.40_{stat} \pm 1.60_{syst}$	$3.3 \times 10^{-7}$
$B^0 \rightarrow \mu^+\mu^-$	$4 \times 10^{-3}$	0	$0.49 \pm 0.19$	$18.8 \pm 0.28_{stat} \pm 2.00_{syst}$	$2.0 \times 10^{-7}$
$B^0 \rightarrow e^\pm\mu^\mp$	—	0	$0.51 \pm 0.17$	$18.3 \pm 0.38_{stat} \pm 1.50_{syst}$	$2.1 \times 10^{-7}$

Table 1: Summary of analysis.  $N_{exp}$  is the number of expected signal events assuming a branching fraction of  $10^{-15}$ .  $N_{obs}$  is the number of observed events in the signal box.  $N_{BG}$  is the expected number of background events in the signal box.

## 4 Results

A summary of the BaBar preliminary results for the rare leptonic B decays are given in table 2 in comparison with CLEO and Belle results.

Mode	CLEO	Belle	Babar
$\mathcal{B}(B^- \rightarrow K^- \nu \bar{\nu})$	$2.4 \times 10^{-4}$	-	$9.4 \times 10^{-5}$
$\mathcal{B}(B^0 \rightarrow e^+e^-)$	$8.3 \times 10^{-7}$	$6.3 \times 10^{-7}$	$3.3 \times 10^{-7}$
$\mathcal{B}(B^0 \rightarrow \mu^+\mu^-)$	$6.1 \times 10^{-7}$	$2.8 \times 10^{-7}$	$2.0 \times 10^{-7}$
$\mathcal{B}(B^0 \rightarrow e^\pm\mu^\mp)$	$15.0 \times 10^{-7}$	$9.4 \times 10^{-7}$	$2.1 \times 10^{-7}$
Luminosity	$9.1 \text{ fb}^{-1}$	$21.3 \text{ fb}^{-1}$	$54.4 \text{ fb}^{-1}$

Table 2: Summary of BaBar, CLEO and Belle results for rare leptonic B decay.

## References

- [1] G. Buchalla, G. Hiller and G. Isidori, Phys. Rev. D **63**, 014015 (2001); hep-ph/0006136.
- [2] P. Colangelo *et al.* Phys. Lett. **B395**, 339-344, (1997); hep-ph/9610297.
- [3] T. E. Browder *et al.* [CLEO Collaboration], Phys. Rev. Lett. **86**, 2950 (2001).
- [4] Y. Grossman, Z. Ligeti and E. Nardi, Nucl. Phys. **B465**, 369-398 (1996); hep-ph/9510378.
- [5] K. Leroux and D. London, Phys. Lett. **B526**, 97-103, (2002); hep-ph/0111246.
- [6] CLEO Collaboration, T. Bergfeld *et al.*, Phys. Rev. D **62**, 0991102(R) (2000)
- [7] BELLE Collaboration, K. Abe *et al.*, BELLE-CONF-0127 (2001)
- [8] H. E. Logan, U. Nierste. Nucl.Phys. **B586**, 39-55 (2000); hep-ph/0004139.

- [9] M. Gronau and D. London, Phys. Rev. D **55**, 2845 (1997); hep-ph/9608430.
- [10] K.S. Babu, C. Kolda. Phys. Rev. Lett. **84**, 228-231 (2000); hep-ph/9909476. C. Bobeth, T. Ewerth, F. Kruger and J. Urban, Phys. Rev. D **64** 074014 (2001); hep-ph/0204225.